Characterization of stability of benchmark organic photovoltaic films after proton and electron bombardments

Jérémy Barbé, Harrison K. H. Lee, Hiroyuki Toyota, Kazuyuki Hirose, Shin-ichiro Sato, Takeshi Ohshima, Keith C. Heasman, and Wing C. Tsoi

Citation: Appl. Phys. Lett. **113**, 183301 (2018); doi: 10.1063/1.5046829
View online: https://doi.org/10.1063/1.5046829
View Table of Contents: http://aip.scitation.org/toc/apl/113/18
Published by the American Institute of Physics

Characterization of stability of benchmark organic photovoltaic films after proton and electron bombardments

Jérémy Barbé,[1,a)] Harrison K. H. Lee,[1,a)] Hiroyuki Toyota,[2] Kazuyuki Hirose,[2] Shin-ichiro Sato,[3] Takeshi Ohshima,[3] Keith C. Heasman,[4] and Wing C. Tsoi[1,b)]
[1]*SPECIFIC, College of Engineering, Swansea University, Bay Campus, Fabian Way, Swansea SA1 8EN, United Kingdom*
[2]*Japan Aerospace Exploration Agency, 3-1-1 Yoshinodai, Chuo-ku, Sagamihara, Kanagawa 252-5210, Japan*
[3]*National Institutes for Quantum and Radiological Science and Technology, 1233 Watanuki-machi, Takasaki, Gunma 370-1292, Japan*
[4]*Ion Beam Centre, Advanced Technology Institute, University of Surrey, Guildford, Surrey GU2 7XH, United Kingdom*

(Received 2 July 2018; accepted 15 October 2018; published online 29 October 2018)

Organic solar cells have attractive potential for space applications as they have very high specific power (power generated per weight) and ultra-high flexibility (to reduce stowed volume). However, one critical issue is whether they are stable under the harsh space environment, particularly their stability under high energy, high flux, electron and proton bombardment. In this paper, the stability of benchmark organic photovoltaic layers under proton bombardment (150 keV with a fluence of $1 \times 10^{12}/cm^2$) and electron bombardment (1 MeV with a fluence of $1 \times 10^{13}/cm^2$) under vacuum is investigated. Raman spectroscopy, photoluminescence spectroscopy, and optical reflectance spectroscopy are applied to study their chemical/structural, photo-chemical/morphological, and optical stability after the bombardments. The results show that all the benchmark organic photovoltaic films are stable under the radiation, implying that organic solar cells could be feasible for space applications. *Published by AIP Publishing*. https://doi.org/10.1063/1.5046829

Organic photovoltaics (OPV) have attractive potential for space applications because they have super-high specific power (power generated per weight: kW/kg) and ultra-high flexibility (roll-able to reduce stowed volume). Both properties are key parameters for space applications, which can reduce the launching costs significantly. NASA has recently demonstrated "Roll-Out of Solar Arrays (ROSA)," which is 20% lighter and 4 times smaller in volume than rigid solar panels.[1] It has been demonstrated that OPV can have a specific power of 10 kW/kg (under AM1.5G illumination),[2] which is much higher than traditional inorganic SCs [≈0.5 kW/kg under AM0 (solar spectrum in space)]. It is important to note that the value of 10 kW/kg is based on an OPV material system with low power conversion efficiency (PCE). Therefore, with state-of-the-art OPV materials with PCE as high as 15%,[3] significantly higher specific power should be achievable. It has also been demonstrated that OPV can reversibly attain tensile strains of more than 300% on an elastomeric support,[2] which makes them much more flexible than inorganic SCs. In 2018, it is reported that OPV were launched to near-space altitude (the stratospheric mission OSCAR) with some encouraging initial results on their stability.[4]

However, there are a number of issues before OPV are feasible for space applications, which include their AM0 PCE, their thermal stability under extreme temperatures cycling, and critically their radiation stability (under high energy photons and particle bombardment). In 2014, Guo *et al*. reported P3HT:$PC_{61}BM$ OSC with an AM0 PCE of ≈1.9% (≈88% of its AM1.5G PCE), and the AM0 PCE maintains quite well even under higher suns (3.3 suns AM0 PCE ≈80% of its 1 sun AM0 PCE) and high temperature (AM0 PCE at 80 °C is about 5% higher than AM0 PCE at 25 °C).[5] Note that though the AM0 PCE seems quite low, the measurement was based on an old OPV system with low AM1.5G PCE, but for state-of-the-art OPV with AM1.5G PCE up to 15%, it would be possible to achieve AM0 PCE >13% (assuming AM0 PCE also ≈88% that of its AM1.5G PCE). In stratospheric mission OSCAR, a set of OPV devices was launched to an altitude of 32 km where electromagnetic radiation (1349 $W\,m^{-2}$) is very similar to outer space (1366.1 $W\,m^{-2}$).[4] The devices survived 3 h of stratospheric flight with minor loss in performance. However, at this altitude, OPV devices did not experience significant radiation from charged particles because of the shielding provided by the earth's magnetic field. In 2018, we have demonstrated that benchmark OPV can maintain PCE under extreme and rapid thermal cycling between −100 °C and 80 °C for 50 cycles.[6] These results show that OPV are promising for space applications.

In terms of high energy photon bombardments, some studies have shown that a high dose of high energy X-rays can reduce charge extraction from the active layer to the electron transporting layer (ETL)/cathode,[7,8] which could be avoided by optimizing the ETL.[9] However, studies on the stability of OPV under high energy electron and proton bombardments are still missing. Here, we performed the electron and proton bombardments on benchmark OPV films. By using Raman spectroscopy (RS), photoluminescence (PL) spectroscopy, and optical reflectance measurements, it is shown that the OPV films do not have significant degradation after the

[a)]J. Barbé and H. K. H. Lee contributed equally to this work.
[b)]E-mail: W.C.Tsoi@swansea.ac.uk.

bombardments, implying that OPV could be feasible for space applications.

To study the feasibility of OPV films for space applications, a proton energy of 150 keV with a fluence of $1 \times 10^{12}\,cm^{-2}$ and an electron energy of 1 MeV with a fluence of $1 \times 10^{13}\,cm^{-2}$ were applied. These energies are common in the space environment, and the fluences are in the range of moderate levels.[10,11] The relative damage coefficient (RDC), which is the degree of damage for each energy relative to the damage by 1 MeV electrons (or 10 MeV protons), is not known for OPV. It means that we were not able to calculate the equivalent 1 MeV (10 MeV) electron (proton) fluence for OPV. However, as a reference, we calculated using SPENVIS software that 1 MeV electron bombardment with the fluence of $1 \times 10^{13}\,cm^{-2}$ corresponds to 5 years dose for the silicon cell and 10 years dose for the triple junction cell without cover glass in Low Earth Orbit (LEO).

In this study, four benchmark OPV material systems were studied including a typical polymer:fullerene system, poly[N-9′-heptadecanyl-2,7-carbazole-alt-5,5-(4′,7′-di-2-thienyl-2′,1′,3′-benzothiadiazole)]:[6,6]-Phenyl-C71-butyric acid methyl ester (PCDTBT:$PC_{71}BM$), a high PCE system, Poly[(2,6-(4,8-bis(5-(2-ethylhexyl)thiophen-2-yl)-benzo[1,2-b:4,5-b′]dithiophene))-alt-(5,5-(1′,3′-di-2-thienyl-5′,7′-bis(2-ethylhexyl)benzo[1′,2′-c:4′,5′-c′]dithiophene-4,8-dione)]:$PC_{71}BM$ (PCE12:$PC_{71}BM$), a polymer: non-fullerene acceptor system, PCE12:3,9-bis(2-methylene-(3-(1,1-dicyanomethylene)-indanone))-5,5,11,11-tetrakis(4-hexylphenyl)-dithieno[2,3-d:2′,3′-d′]-s-indaceno[1,2-b:5,6-b′]dithiophene (PCE12:ITIC), and a high PCE small molecule donor: fullerene system, benzodithiophene terthiophene rhodanine:$PC_{71}BM$ (BTR:$PC_{71}BM$). The layer structure is quartz/PEDOT:PSS/OPV layer/PEIE/Ag (mimic device structure). Quartz substrates were used because proton and electron bombardments can darken glass substrates.[12,13]

PCDTBT, PBDB-T, ITIC, and BTR were purchased from 1-Material. $PC_{71}BM$ was purchased from Solenne BV. PEDOT:PSS, Clevios P VP AI 4083, was purchased from Heraeus. PEIE, chlorobenzene, chloroform, and tetrahydrofuran are purchased from Sigma-Aldrich. All materials were used as received. BTR and BTR:$PC_{71}BM$ solutions were dissolved in chloroform, while other systems (both neat and blend) are dissolved in chlorobenzene. The donor:acceptor ratio of the systems BTR:$PC_{71}BM$, PBDB-T:$PC_{71}BM$, and PBDB-T:ITIC is 1:1, while the ratio for PCDTBT:$PC_{71}BM$ is 1:2. Quartz substrates were cleaned sequentially with detergent (Hellmanex), deionized water, acetone, and isopropyl alcohol in an ultrasonic bath. All quartz substrates were cleaned with plasma treatment. PEDOT:PSS was first spin coated onto the substrates followed by a 10 min drying on a hot plate of 150 °C. All active layers are spin coated onto the quartz or PEDOT:PSS coated substrates in a nitrogen filled glovebox. ITIC neat and blend films underwent thermal annealing on a hotplate of 100 °C for 10 min. BTR neat and blend films underwent solvent vapour annealing in a Petri dish with tetrahydrofuran filled in a section. 0.03 wt. % PEIE solution (diluted with ethanol) are spin coated onto the active layers. Finally, 100 nm of Ag were thermally evaporated onto all the samples in an evaporator.

The UV-Vis reflectance spectra were measured in the range of 320–850 nm with a 1 nm step using a Perkin Elmer Lambda 750 spectrophotometer equipped with an integrating sphere. 100% reflectance spectra were measured using quartz substrates coated with silver, while 0% reflectance spectra were recorded by blocking the light beam before it enters the integrating sphere. All samples coated with organic films and silver were measured from the quartz side. The Raman and PL measurements were performed with a Renishaw Invia Raman system in the backscattering configuration. A 532 nm laser and a 50× objective were used (NA: 0.50, spot size $\approx 1\,\mu m$). For micro-Raman measurements, the laser power was varied between 0.03 and 0.3 mW to enhance the signal-to-noise ratio and an acquisition time of 10 s was used. For the micro-PL measurements, a laser power between 0.03 μW and 15 μW and an acquisition time between 1 s and 20 s were used. 1800 l/mm and 300 l/mm gratings were used for the Raman and PL measurements, respectively.

The proton beam irradiation was carried out at the Surrey Ion Beam Centre in UK. Sample loading was carried out in a class 100 clean room. The organic PV samples were mounted two at a time onto 3 in. silicon wafers onto 4 in. support plates which were inserted into a carousel wheel in the sample chamber. The samples were held in position using tungsten wire clips to the edge of the sample. The clip allowed charge to be conducted away from the sample. In total, 14 samples were mounted onto seven plates. Samples were loaded in a 7°/0° tilt/twist orientation to the incident beam and implanted under vacuum ($2.3 \pm 0.2 \times 10^{-6}$ mbar). A Danfysik 1090 low energy high current implanter was used to implant 150 keV protons into the samples (from the Silver side). The total fluence of each implant was $1 \times 10^{12}/cm^2$. The fluence rate was controlled to $3 \times 10^{10}/cm^2\,s$, meaning that each implant lasted 33 s.

The electron beam irradiation was carried out at Takasaki Advanced Radiation Research Institute of National Institutes for Quantum and Radiological Science and Technology in Japan. The samples were fixed on a water cooled stage by carbon double-sided tapes with high thermal conductivity. In order to prevent physical damage to the layers, the samples were placed with the OPV layers facing up and the glass substrates down. To eliminate the influence of moisture and oxygen in the atmosphere, the samples were placed in a chamber which was evacuated by an oil-sealed rotary pump during the irradiation. The samples were irradiated (from the Silver side) with a 1.0-MeV electron beam with a fluence rate of $1.0 \times 10^{11}/cm^2\,s$ for 100 s, which resulted in a total fluence of $1.0 \times 10^{13}/cm^2$. The temperature of the samples should have been kept below 35 °C from the past experience during the irradiation.

To study the effect of the proton and electron bombardments on the chemical stability of the OPV films in the device structure, RS was performed before and after the bombardments. Note that all the samples were first characterized fresh, bombarded with protons and characterized, and then bombarded with electrons and characterized again. RS is a simple but powerful technique which can be used to probe structural/chemical degradation of OPV films.[14,15] Besides, since the excitation laser beam can pass through the quartz side to collect the Raman scattered light, it can be utilized to probe embedded PV films in a device structure.[16,17]

Figure 1 shows the normalized Raman spectra of the four benchmark type OPV films in the device structure, before and after the proton and electron bombardments. The spectral region of ≈1300–1600 cm^{-1} could be attributed to C-C and C=C vibrational modes of the molecules.[14,18] For the PCDTBT:$PC_{71}BM$ film [Fig. 1(a)], the Raman spectrum is dominated by the PCDTBT [see Fig. S1(a) for the Raman spectrum of the neat PCDTBT film], with a small peak at ≈1567 cm^{-1} which can be attributed to $PC_{71}BM$ [see Fig. S1(b) for the Raman spectrum of the neat $PC_{71}BM$ film]. Therefore, in this case, RS can be used to study the stability of the electron donor and acceptor simultaneously. As there is no change in the Raman spectrum after the bombardments, it agrees well that there is no degradation for both the electron donor and acceptor. To further support it, Fig. S1(b) shows that there is no change in the Raman spectrum for neat $PC_{71}BM$ film after the bombardments. For the PCE12:$PC_{71}BM$ film [Fig. 1(b)], the Raman spectrum is dominated by PCE12 [see Fig. S1(c) for the Raman spectrum of the neat PCE12 film] with no observable Raman signal from $PC_{71}BM$. As there is no change in the Raman spectrum, it is consistent with no degradation of PCE12. For PCE12:ITIC [Fig. 1(c)], the Raman spectrum is also dominated by PCE12 while the 1600 cm^{-1} peak can be assigned to ITIC [see Fig. S1(d) of the Raman spectrum of the neat ITIC film]. The similar Raman spectrum after the bombardments is again consistent with no degradation of both PCE12 and ITIC. Figure S1(d) shows that there is no change in the Raman spectrum of the neat ITIC film after the bombardments, which further supports that ITIC is stable. For BTR:$PC_{71}BM$ [Fig. 1(d)], the Raman spectrum is dominated by BTR [see Fig. S1(e) for the Raman spectrum of the neat BTR film], which does not show any change after the bombardments, consistent with its good stability toward the radiations. In brief, all the OPV films are chemically/structurally stable during the bombardments. Note that the magnitude of all the Raman spectra is also very similar before and after the bombardments (not shown), which further supports the structural/chemical stability.

To study the effect of the proton and electron bombardment on the photo-chemical stability of the films in the device structure, PL spectroscopy was performed before and after the bombardments. PL spectroscopy is a simple technique which is powerful to probe the photochemical degradation of OPV films.[19–21] Besides, since the excitation source is a light beam, it can be easily utilized to probe the embedded films in a device structure.

Figure 2 shows the normalized PL spectra of the four benchmark OPV films in the device structure, before and after the proton and electron bombardments. For PCDTBT:$PC_{71}BM$ [Fig. 2(a)], there is a PL peak at 713 nm, a shoulder at ≈787 nm, and significant PL at 850 nm. The spectral shape is similar to the PL spectrum of the neat $PC_{71}BM$ film [see Fig. S2(a) for the PL spectrum of the neat $PC_{71}BM$ film], which has a PL peak at 715 nm, a shoulder at ≈783 nm, and significant PL at 850 nm. In contrast, the PL spectrum of the neat PCDTBT film [see Fig. S2(b) for the PL spectrum of the neat PCDTBT film] only has a peak at 707 nm with very weak PL at 850 nm. Therefore, the PL spectrum of PCDTBT:$PC_{71}BM$ is dominated by $PC_{71}BM$ (likely with some PL from PCDTBT), which shows no photochemical degradation after the bombardments. Figure S2(b) shows that the PL spectrum of the neat PCDTBT film does not change after the bombardments, supporting that the PCDTBT in the blend should also be photochemically stable against the bombardments. For the PCE12:$PC_{71}BM$ film [Fig. 2(b)], the PL spectrum has a main peak at 725 nm, shoulders at ≈681 nm and >784 nm, and significant PL at 850 nm. The PL spectrum can be attributed to a mixture of the PL spectrum of the PCE12 film [see Fig. S2(c), a peak at 690 nm, a shoulder at 736 nm] and $PC_{71}BM$ film [see Fig. S2(a), a PL peak at 715 nm, a shoulder at ≈783 nm, with significant PL at 850 nm]. Therefore, in this case, the PL spectrum of the blend film can be used to study the photochemical

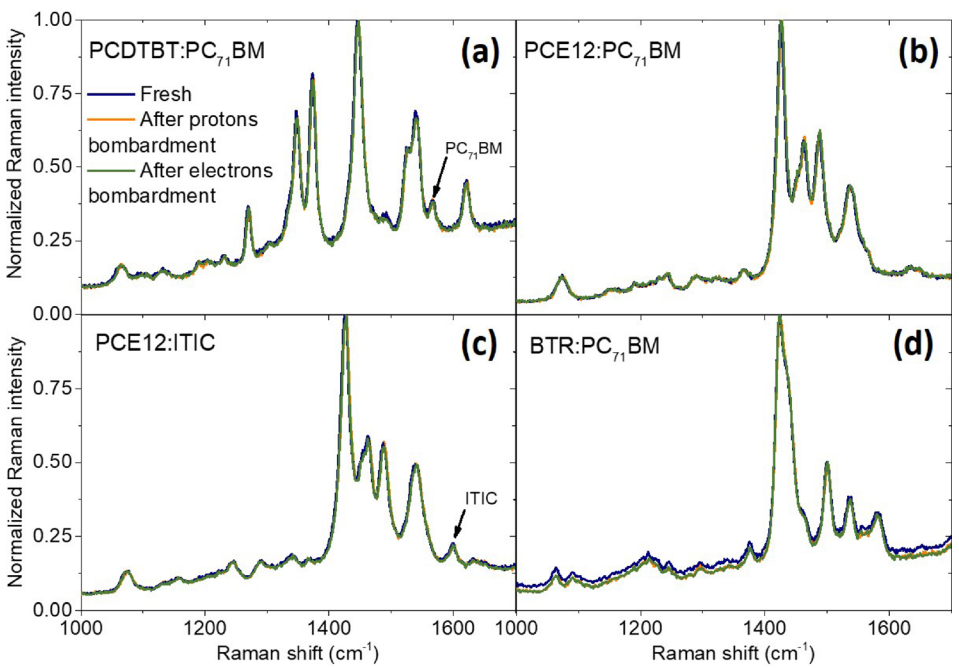

FIG. 1. Normalized Raman spectra of the (a) PCDTBT:$PC_{71}BM$ film, (b) PCE12:$PC_{71}BM$ film (c) PCE12:ITIC film, and (d) BTR:$PC_{71}BM$ film, in the device structure.

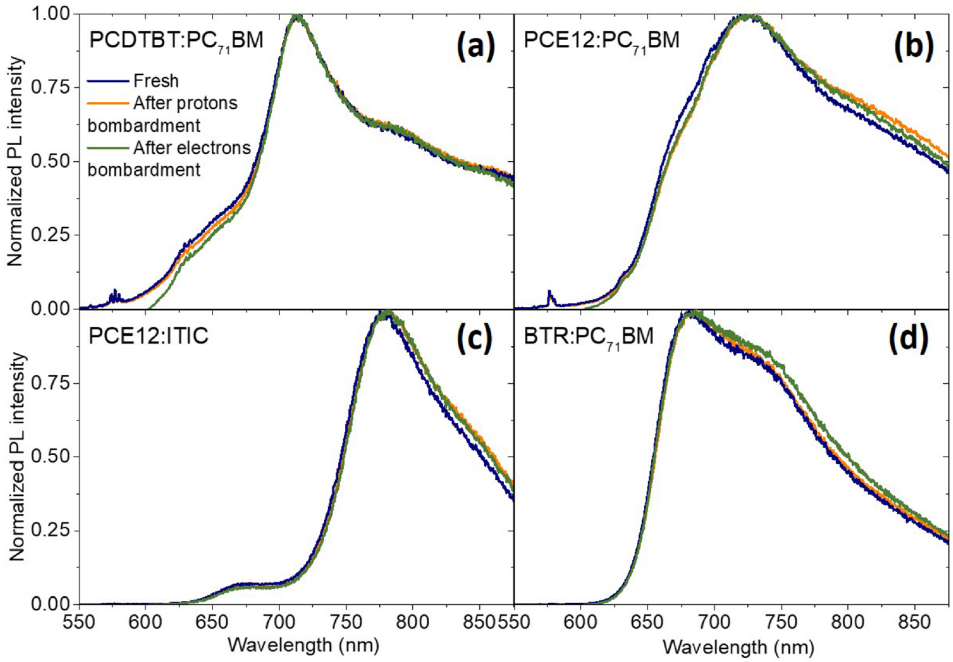

FIG. 2. Normalized PL spectrum of the (a) PCDTBT:$PC_{71}BM$ film, (b) PCE12:$PC_{71}BM$ film, (c) PCE12:ITIC film, and (d) BTR:$PC_{71}BM$ film, in the device structure.

stability of both the electron donor and acceptor simultaneously. As there is no considerable change in the PL spectrum of the PCE12:$PC_{71}BM$ film, PCE12 and $PC_{71}BM$ are photo-chemically stable against the bombardments. For the PCE12:ITIC film [see Fig. 2(c)], the PL spectrum has a peak at 781 nm, a shoulder at ≈672 nm, and significant PL at 850 nm. The PL spectrum is dominated by ITIC [see Fig. S2(d), a PL peak at 784 nm and significant PL at 850 nm] with some contributions from PCE12 [see Fig. S2(c), a peak at 690 nm]. As there is no change in the PL spectrum of the blend film after the bombardments, both the PCE12 and ITIC are stable. For the BTR:$PC_{71}BM$ film [see Fig. 2(d)], the PL spectrum has a peak at 682 nm, a shoulder at 728 nm, and some PL at 850 nm. None of the PL spectra of neat BTR [see Fig. S2(e), peaks at 745 nm and 719 nm] and neat $PC_{71}BM$ [see Fig. S2(a), peaks at 715 nm] have a peak at 682 nm, which implies that BTR and $PC_{71}BM$ could disturb each other's PL properties when blending them. Nevertheless, there is no degradation in the PL spectrum of the BTR:$PC_{71}BM$ film after the bombardments. In brief, the PL data agree well that all the OPV films are photo-chemically stable against proton and electron radiations. The magnitude of the PL spectra for all the OPV films is also very similar before and after the bombardments (not shown here), which further supports no considerable photochemical degradation after the bombardments. Furthermore, since the magnitude of PL can also be strongly affected by the degree of mixing between the donor and acceptor, the PL data also indicate that there is no

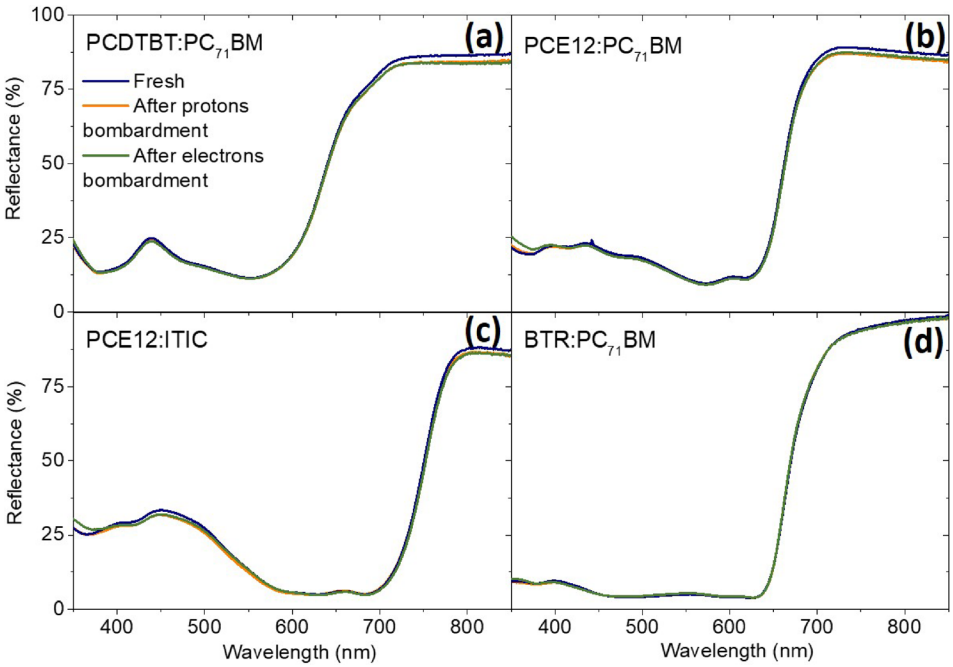

FIG. 3. Diffuse reflectance spectra of the (a) PCDTBT:$PC_{71}BM$ film, (b) PCE12:$PC_{71}BM$ film, (c) PCE12:ITIC film, and (d) BTR:$PC_{71}BM$ film, in the device structure.

considerable morphological change of the OPV films after the bombardments.

Finally, diffuse reflectance spectroscopy was performed before and after the bombardments. Diffuse reflectance spectroscopy can be used to gain information on the absorption of the OPV films in the device structure, which could not be measured by using typical absorbance measurements as the silver electrode is not transparent to the light beam. Figure 3 shows the diffuse reflectance spectra of the four benchmark OPV films in the device structure, before and after the proton and electron bombardments. Basically, all the reflectance spectra could be attributed to a mixture of reflectance spectra of the donors and acceptors [see Figs. S3(a)–S3(e) for the reflectance spectra of the neat films]. Therefore, this approach allows probing the optical degradation of both the donors and the acceptors in the blend films simultaneously. It is clear that there is no significant change in all the diffuse reflectance spectra for all the OPV films, which is consistent with no optical degradation after the bombardments.

The optical techniques applied here can be highly sensitive to crystallinity or conformational changes in the organic films. It has been shown that for BTR:$PC_{71}BM$ films, even subtle changes in molecular conformation and photo-physical/chemical properties after degradation can be detected by these three techniques.[15] Briefly, UV-Vis showed photobleaching of the films, Raman showed changes in peaks intensity and position, and PL showed red-shifting, decreased intensity, and disappearance of the shoulder peaks after aging. In another work, by using UV-Vis and RS, it is shown that decreased mobility and increased threshold voltage of an organic transistor after neutron irradiation can be correlated with a decrease in the degree of molecular order (broadening of Raman peaks) and increased energetic disorder (slight blue-shift of the main absorption feature).[22] These studies show that these optical characterization techniques provide a sensitive evaluation of the structural/chemical changes in the blend layer. The fact that no peak broadening/shift/intensity change was observed in the Raman, PL, and UV-Vis spectra (even small) is a strong indication that the four OPV films studied here remain stable after the proton and electron bombardment.

In summary, four benchmark OPV films were bombarded by high energy, moderate fluence protons and electrons. By applying RS, PL spectroscopy, and optical reflectance spectroscopy, it is shown that the OPV films are chemically/structurally, photo-chemically/morphological and optically stable against the proton and electron irradiations, implying that OPV (and organic electronics) could be used for space applications. Further works will be on AM0 PCE of the OPV before and after the bombardments, with higher fluences and a wider range of energies.

See supplementary material for Raman spectra, photoluminescence spectra and reflectance spectra of neat films before and after proton and electron bombardment.

The authors acknowledge funding from the EPSRC (Grant No. EP/M025020/1), Welsh Assembly Government funded Ser Cymru Solar Project.

[1]See https://en.wikipedia.org/wiki/Roll_Out_Solar_Array for information about Roll Out Solar Array (ROSA).
[2]M. Kaltenbrunner, M. S. White, E. D. Głowacki, T. Sekitani, T. Someya, N. S. Sariciftci, and S. Bauer, Nat. Commun. **3**, 770 (2012).
[3]X. Che, Y. Li, Y. Qu, and S. R. Forrest, Nat. Energy **3**, 422 (2018).
[4]I. Cardinaletti, T. Vangervena, S. Nagels, R. Cornelissen, D. Schreurs, J. Hruby, J. Vodnik, D. Devisscher, J. Kesters, J. D'Haen, A. Franquet, V. Spampinato, T. Conard, W. Maes, W. Deferme, and J. V. Manca, Sol. Energy Mater. Sol. Cells **182**, 121 (2018).
[5]S. Guo, C. Brandt, T. Andreev, E. Metwalli, W. Wang, J. Perlich, and P. Müller-Buschbaum, ACS Appl. Mater. Interfaces **6**, 17902 (2014).
[6]H. K. H. Lee, J. R. Durrant, Z. Li, and W. C. Tsoi, J. Mater. Res. **33**, 1902–1908 (2018).
[7]A. Kumar, R. Devine, C. Mayberry, B. Lei, G. Li, and Y. Yang, Adv. Funct. Mater. **20**, 2729 (2010).
[8]A. K. Thomas, C. J. Kouhestani, and J. K. Grey, Sol. Energy Mater. Sol. Cells **160**, 85 (2017).
[9]A. Kumar, N. Rosen, R. Devine, and Y. Yang, Energy Environ. Sci. **4**, 4917 (2011).
[10]S. R. Messenger, G. P. Summers, E. A. Burke, R. J. Walters, and M. A. Xapsos, Prog. Photovoltaics: Res. Appl. **9**, 103 (2001).
[11]D. J. Curtin and R. L. Statler, IEEE Trans. Aerosp. Electron. Syst. **AES-11**, 499–513 (1975).
[12]Y. Miyazawa, M. Ikegami, T. Miyasaka, T. Ohshima, M. Imaizumi, and K. Hirose, in IEEE 42nd Photovoltaic Specialist Conference (PVSC) (2015).
[13]J. Čermák, L. Mihai, D. Sporea, Y. Galagan, J. Fait, A. Artemenko, P. Štenclová, B. Rezek, M. Straticiuc, and I. Burducea, Sol. Energy Mater. Sol. Cells **186**, 284–290 (2018).
[14]M. J. Newman, E. M. Speller, J. Barbé, J. Luke, M. Li, Z. Li, Z.-K. Wang, S. M. Jain, J.-S. Kim, H. K. H. Lee, and W. C. Tsoi, Sci. Technol. Adv. Mater. **19**, 194 (2018).
[15]J. R. Hollis, J. Wade, W. C. Tsoi, Y. Soon, J. Durrant, and J.-S. Kim, J. Mater. Chem. A **2**, 20189 (2014).
[16]K. E. A. Hooper, H. K. H. Lee, M. J. Newman, S. Meroni, J. Baker, T. M. Watson, and W. C. Tsoi, Phys. Chem. Chem. Phys. **19**, 5246 (2017).
[17]J. Barbé, V. Kumar, M. J. Newman, H. K. H. Lee, S. M. Jain, H. Chen, C. Charbonneau, C. Rodenburg, and W. C. Tsoi, Sustainable Energy Fuels **2**, 905 (2018).
[18]W. C. Tsoi, D. T. James, J. S. Kim, P. G. Nicholson, C. E. Murphy, D. D. C. Bradley, J. Nelson, and J.-S. Kim, J. Am. Chem. Soc. **133**, 9834 (2011).
[19]S. Chambon, Ph.D. thesis, Universite Blaise Pascal, 2006.
[20]K. Norrman, N. B. Larsen, and F. C. Krebs, Sol. Energy Mater. Sol. Cells **90**, 2793 (2006).
[21]M. Manceau, A. Rivaton, J.-L. Gardette, J.-L. Guillerez, and N. Lemaitre, Sol. Energy Mater. Sol. Cells **95**, 1315 (2011).
[22]G. M. Paternò, V. Robbiano, K. J. Fraser, C. Frost, V. Garciá Sakai, and F. Cacialli, Sci. Rep. **7**, 41013 (2017).